Transactions of the Korean Nuclear Society Autumn Meeting
Goyang, Korea, October 24-25, 2019

Heat structure coupling of MARS-KS and STAR-CCM+ for wall condensation in the presence of non-condensable gases containing light gas

Chang Won Lee*, Jin-Seong Yoo, Hyoung Kyu Cho
Dept. of nuclear engineering, Seoul National Univ., 1 Gwanak-ro, Gwanak-gu, Seoul 08826
**Corresponding author: szilard94@snu.ac.kr*

1. Introduction

During a postulated severe accident, thermal hydraulic phenomena such as condensation/re-evaporation, hydrogen stratification and hydrogen combustion occur inside the NPP containment. Therefore, large-scale containment experiments and analysis using lumped parameter codes and CFD codes have been conducted to guarantee the safety of containment [1, 2]. However, due to the inherent characteristics of LP codes, there are limitations in analyzing multidimensional flows and local gas concentrations are difficult to obtain [3]. CFD codes have the advantage of being useful in three-dimensional fluid simulations, but because of their high computational cost, CFD codes generally have limitations for standalone analysis of large containment buildings. Thus, LP-CFD code coupling and the analysis using coupled code have been performed [4, 5].

In this study, a code coupling system for LP code and commercial CFD code, MARS-KS and STAR-CCM+, was established. The data exchange between codes is achieved through socket communication [6]. For that, a socket communication subroutine was added in MARS-KS, and a macro script for operating STAR-CCM+ was written. With the coupled code, an analysis of the condensation heat transfer experiment was conducted to validate the coupled code.

2. Computational analysis

2.1 Code coupling method

Code coupling using socket communication was performed for the condensation heat transfer analysis. Socket communication is one of the most commonly used data exchanging methods for server networking. This method was chosen because it facilitates the data transfer between codes on different operation systems, for example, coupling between a code on Windows and the other on Linux. As shown in Fig. 1, the socket servers were established in MARS-KS on Windows and STAR-CCM+ on Linux respectively, and servers in an interface program were connected to each servers. For that, socket communication subroutines in MARS-KS were added and modified. A JAVA macro was written for socket communication in STAR-CCM+ code.

In this study, heat transfer was calculated with code coupling via heat structure without flow parameter exchange. For that, the explicit-coupling method was used, in which two codes independently performed thermal-hydraulic calculations and then exchanged data to change the boundary conditions of the other. At the end of every time step, surface temperature calculated by MARS-KS and boundary heat flux calculated by STAR-CCM+ were exchanged. In MARS-KS, the heat structure surface heat flux is set to be input as a general table [7]. The interface program is configured so that MARS-KS receives that of STAR-CCM + and the two codes use the same time step.

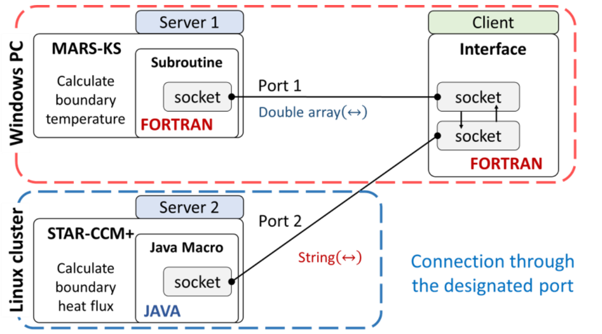

Fig. 1. System & CFD code coupling with socket communication scheme

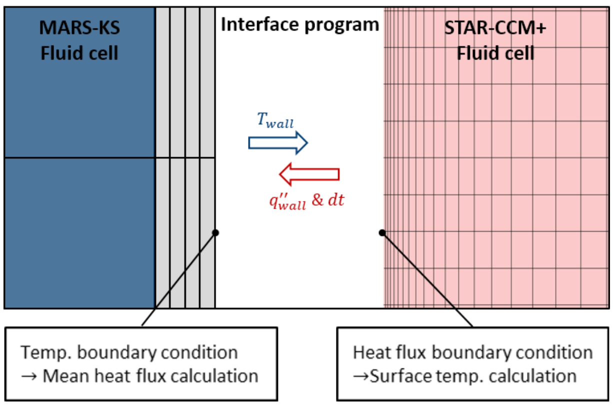

Fig. 2. Diagram of the heat structure coupling method

2.2 Condensation simulation results

To verify and validate the coupled code, the CONAN experiment, which is a separate effect test for condensation heat transfer, was analyzed [8].

The inlet and outlet conditions of the primary and secondary sides are used as shown in Table I. The computational domain was determined as shown in Fig. 3. The primary side where multidimensional two-phase flow is formed was analyzed using commercial CFD code, STAR-CCM+, and the secondary side was analyzed using MARS-KS which can properly simulate convective heat transfer phenomena in the coolant channel if a multi-dimensional effect is insignificant. The aluminum plate where the heat transfer occurred was simulated with the heat structure of MARS-KS code. As the CFD analysis grid (Fig. 4 (a)), 400,000 grids were generated and y + was kept below 1. In the case of P05-T40-V06-H90, a helium rich condition, the reverse flow occurred at the exit of the geometry. For that reason, the geometry was modified to reduce the outlet area gradually as in the experimental apparatus, and the number of grids increased to 600,000 as illustrated in Fig. 4 (b). The realizable k-e model was used as a turbulent model, and the wall condensate was simulated using a fluid film model of STAR-CCM + code [9].

Table. I. The boundary conditions of the CONAN test

<table>
<tr><td rowspan="4">P20-T50-V30-H08</td><td colspan="4">$\dot{m}_{sec}$ $[kg/s]$</td><td colspan="4">$T_{in,sec}$ [°C]</td><td colspan="4">$T_{out,sec}$ [°C]</td></tr>
<tr><td colspan="4">0.9536</td><td colspan="4">50.2</td><td colspan="4">53.6</td></tr>
<tr><td colspan="3">$V_{out,pri}[m/s]$</td><td colspan="3">$T_{in,pri}$ [°C]</td><td colspan="3">$Y_{in,air}$ $[-]$</td><td colspan="3">$Y_{in,He}[-]$</td></tr>
<tr><td colspan="3">3.11</td><td colspan="3">92.0</td><td colspan="3">0.402</td><td colspan="3">0.005</td></tr>
<tr><td rowspan="4">P20-T50-V30-H65</td><td colspan="4">$\dot{m}_{sec}$ $[kg/s]$</td><td colspan="4">$T_{in,sec}$ [°C]</td><td colspan="4">$T_{out,sec}$ [°C]</td></tr>
<tr><td colspan="4">1.0832</td><td colspan="4">49.7</td><td colspan="4">52.7</td></tr>
<tr><td colspan="3">$V_{out,pri}[m/s]$</td><td colspan="3">$T_{in,pri}$ [°C]</td><td colspan="3">$Y_{in,air}$ $[-]$</td><td colspan="3">$Y_{in,He}[-]$</td></tr>
<tr><td colspan="3">3.06</td><td colspan="3">89.1</td><td colspan="3">0.223</td><td colspan="3">0.056</td></tr>
<tr><td rowspan="4">P05-T40-V06-H62</td><td colspan="4">$\dot{m}_{sec}$ $[kg/s]$</td><td colspan="4">$T_{in,sec}$ [°C]</td><td colspan="4">$T_{out,sec}$ [°C]</td></tr>
<tr><td colspan="4">0.7232</td><td colspan="4">39.9</td><td colspan="4">40.9</td></tr>
<tr><td colspan="3">$V_{out,pri}[m/s]$</td><td colspan="3">$T_{in,pri}$ [°C]</td><td colspan="3">$Y_{in,air}$ $[-]$</td><td colspan="3">$Y_{in,He}[-]$</td></tr>
<tr><td colspan="3">~0.6</td><td colspan="3">76.9</td><td colspan="3">0.429</td><td colspan="3">0.093</td></tr>
<tr><td rowspan="4">P05-T40-V06-H90</td><td colspan="4">$\dot{m}_{sec}$ $[kg/s]$</td><td colspan="4">$T_{in,sec}$ [°C]</td><td colspan="4">$T_{out,sec}$ [°C]</td></tr>
<tr><td colspan="4">0.6901</td><td colspan="4">40.5</td><td colspan="4">41.7</td></tr>
<tr><td colspan="3">$V_{out,pri}[m/s]$</td><td colspan="3">$T_{in,pri}$ [°C]</td><td colspan="3">$Y_{in,air}$ $[-]$</td><td colspan="3">$Y_{in,He}[-]$</td></tr>
<tr><td colspan="3">~0.6</td><td colspan="3">71.1</td><td colspan="3">0.190</td><td colspan="3">0.219</td></tr>
</table>

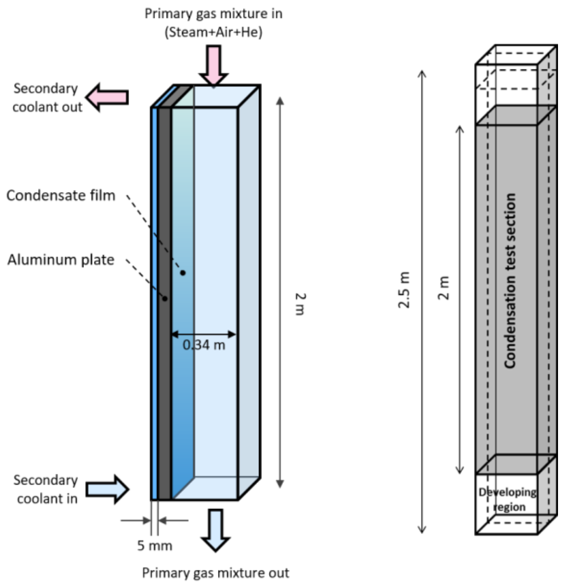

Fig. 3. Sketch of the CONAN facility test section and computational domain of CFD analysis

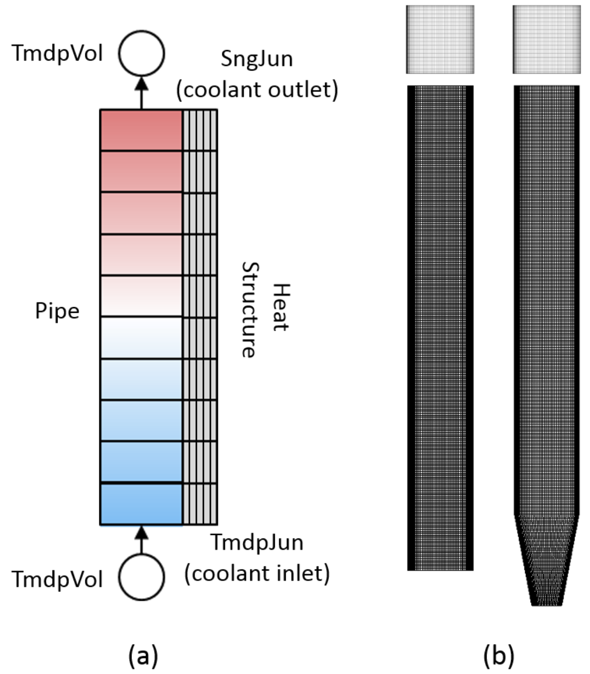

Fig. 4. Sketch of node and meshes of MARS-KS/STAR-CCM+ coupled code analysis
(a: MARS-KS, b: STAR-CCM+)

For the wall temperature boundary condition of CFD code, the field function was used by interpolating the temperature calculated in the MARS-KS code. The nodalization for the MARS-KS analysis is shown in Fig. 4. It consists of a pipe that flows cooling water and a heat structure that simulates an aluminum plate. For the right boundary condition of the heat structure, the average heat flux at the height of each node was calculated by averaging the condensation heat flux delivered from CFD. In order to evaluate the analysis results of the coupled codes, the results were compared with the results of CONAN test and the CFD standalone analysis as illustrated in Fig. 5 and 6. It was observed that the results of the coupled code showed good agreements with the local condensation heat fluxes of the stand-alone CFD analysis and the experiment results. The total condensation heat transfer rate at the condensation surface was predicted within ±20% of the experimental results as shown in Fig. 7. The low overall condensation heat transfer rates under the forced convective condensation conditions are due to the limitations assumed for laminar flow in the fluid film model of the STAR-CCM+. In the forced convective condensation case, the condensation film Reynolds number is about 150, which is the wavy film range. Therefore, if the laminar flow assumption is applied, the thermal resistance of the condensation film is evaluated relatively large.

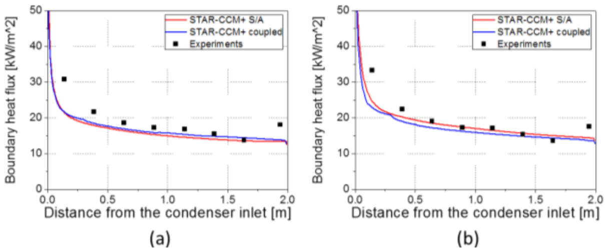

Fig. 5. Comparison between calculated and experimental heat fluxes: forced convective condensation
(a: P20-T50-V30-H08, b: P20-T50-V30-H65)

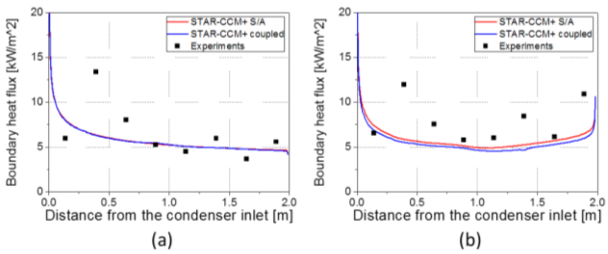

Fig. 6. Comparison between calculated and experimental heat fluxes: natural convective condensation
(a: P05-T40-V06-H62, b: P05-T40-V06-H90)

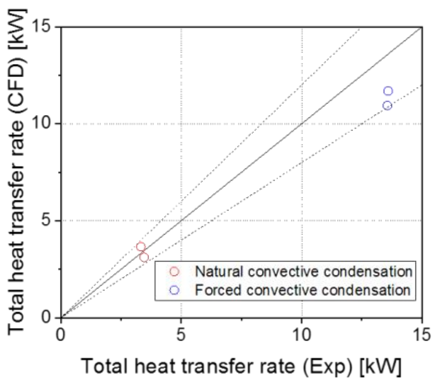

Fig. 7. Comparison of total heat transfer rate between calculated and experimental results

3. Conclusion

In this study, code coupling was performed using socket communication, and condensation heat transfer analysis was conducted with coupled code. For the code coupling, MARS-KS and STAR-CCM+ were used. In order to evaluate the MARS-STAR coupled code, validation was performed against the CONAN experiment containing He for the steam-gas mixture.

Analysis results using the coupled code showed reasonable results compared with CFD standalone analysis and experimental results. However, it can be seen that under forced convective condensation, the condensation heat flux is underestimated because the thermal resistance of the liquid film is incorrectly evaluated. Therefore, it is necessary to quantitatively evaluate and improve the effect of the condensation film model. Nevertheless, it could be confirmed that the coupled code with socket communication can be used to simulate conjugate heat transfer phenomenon including convective and condensation heat transfer in the presence of non-condensable gases. In the future, the coupled code is expected to be used to analyze containment thermal hydraulic phenomena in large containment experiments or a heat exchanger for the containment cooling.

Acknowledgement

This work was supported by the Seoul National University Electric Power Research Institute and the Korea Radiation Safety Foundation (KORSAFE) grant funded by the Korean government (MSIP & NSSC) (Nuclear Safety Research Center Program: 1305011)

REFERENCES

[1] S. Kelm, H. Müller, and H-J. Allelein, A Review of the CFD Modeling Progress Triggered by ISP-47 on Containment Thermal Hydraulics, Nuclear Science and Engineering, 193, 63-80, 2019.

[2] I. Kljenak et al., Simulation of hydrogen deflagration experiment–Benchmark exercise with lumped-parameter codes, Nuclear Engineering and Design, 283, 51-59, 2015.

[3] J. Jeon et al., Identification of hydrogen flammability in steam generator compartment of OPR1000 using MELCOR and CFX codes, Nuclear Engineering and Technology, 2019.

[4] T. Szabó, F. Kretzschmar, and T. Schulenberg, Obtaining a more realistic hydrogen distribution in the containment by coupling MELCOR with GASFLOW, Nuclear Engineering and Design, 269, 330-339, 2014.

[5] T. Bury, Coupling of CFD and lumped parameter codes for thermal-hydraulic simulations of reactor containment, Computer Assisted Methods in Engineering and Science, 20(3), 195-206, 2017.

[6] Yoo, J. S., Choi, D. K., Cho. C. R., Cho, H. K., Coupling of MARS-KS and STAR-CCM+ and Preliminary Calculation for Multi-scale Thermal-hydraulic Analysis, Korean Society for Fluid Machinery, 2019.

[7] Korea Atomic Energy Research Institute, MARS CODE MANUAL, Korea Atomic Energy Research Institute Report, KAERI/TR-3042, 2005.

[8] M. Bucci, Experimental and computational analysis of condensation phenomena for the thermal-hydraulic analysis of LWRs containments, Ph. D. thesis, University of Pisa, 2009.

[9] CD adapco, CD-adapco USER GUIDE STAR-CCM+ Version 13.02, CD-adapco, 2013